Geophys. J. Int. (1989) **98**, 93–106

Crustal structure and possible anisotropy in Turkey from seismic surface wave dispersion

Oznur Y. Mindevalli* and Brian J. Mitchell
Department of Earth and Atmospheric Sciences, Saint Louis University, St Louis, MO 63103, USA

Accepted 1989 January 11. Received 1988 December 22; in original form 1988 March 18

SUMMARY

The velocity structure of two regions of Turkey are determined using single-station measurements of Rayleigh and Love wave group velocities in the period range 8–50 s. A differential inversion scheme yields models for Turkey in which crustal and upper mantle shear-wave velocities are slower than those of most of Europe. Comparisons of upper mantle shear-wave velocities we have obtained with reported P_n velocities leads to Poisson's ratio values in the upper mantle between 0.29 and 0.30 for eastern Turkey and between 0.27 and 0.31 for western Turkey. Crustal velocities are slightly slower and upper mantle velocities are slightly faster in western Turkey than in eastern Turkey. The crust–mantle boundary obtained in our studies is gradational, but if a shear velocity of 4.2 km s^{-1} is taken to define the upper mantle then the crust appears to be about 40 km thick throughout all of Turkey. A sharp crust–mantle boundary may occur, but cannot be resolved. The data of this study require neither a low-velocity zone in the upper mantle nor polarization anisotropy in the crust or upper mantle. Azimuthal variations of Rayleigh and Love wave group velocities in western Turkey are consistent with velocities predicted by an azimuthally anisotropic upper crust in which vertical cracks are orientated in an approximate E–W direction. This interpretation is consistent with geological information, fault-plane solutions, lineations mapped from satellite observations, and reported heat flow values, but the possibility that these variations are caused by lateral changes of velocity in the crust of western Turkey cannot be completely ruled out at the present time.

Key words: crustal structure, anisotropy, Turkey, dispersion

INTRODUCTION

The Turkish subplate lies between the northward moving African and Arabian plates to the south, the Eurasian plate or Black Sea subplate to the north, and the Aegean plate to the west. Like other continental plates and fragments in the eastern Mediterranean, it is relatively rigid and is surrounded by wide deforming zones along which motion occurs (Jackson & McKenzie 1988).

Although much is now known about the tectonics of this region (e.g. McKenzie 1972; Le Pichon & Angelier 1979; Rotstein and Kafka 1982; Kasapoglu & Toksoz 1983; Jackson & McKenzie 1984, 1988; Rotstein & Ben-Avraham 1986), relatively little data have been collected with which to study crust and upper mantle structure, particularly how it might vary across Turkey. Canitez & Toksöz (1980), using travel-time residuals of teleseismically recorded compressional waves, concluded that compressional-wave velocities in the uppermost mantle are 7.9 km s^{-1} in eastern Turkey and 8.1 km^{-1} in western Turkey. Chen, Chen & Molnar (1980), however, concluded that uppermost mantle compressional-wave velocities over a broad region in Turkey are 7.73 km s^{-1} and lie beneath a crust of uniform but poorly determined thickness.

Estimates of crustal thickness have varied widely. Ezen (1983) used Love wave dispersion to infer a thickness of 38 km in northern and eastern Anatolia. Turkelli (1985) determined crustal transfer functions for teleseismic waves and concluded that the crustal thickness beneath Ankara is about 30 km. By contrast, a thickness of 52 km was obtained by Dewey *et al.* (1986) for eastern Turkey using petrological information.

In the present study we use seismic surface waves to study the shear-velocity structure of the crust and upper mantle beneath Turkey. Recent improvements in methods for determining surface-wave group velocities (Russell, Herrmann & Hwang 1984) and in the inversion of those data (Russell 1987; Hwang & Mitchell 1987) should allow us to place greater constraints on crustal and upper mantle velocities, as well as on crustal thickness, than has been previously possible.

Our primary goal is to determine the depth distribution of seismic velocities and their regional variation across Turkey. This information will then allow a comparison with published results for shear velocities in the more stable regions of Eurasia. In addition, since this is a tectonically active region, it is possible that the upper crust is characterized by uniformly orientated cracks, and the upper

* Present address: Middle East Technical University, Ankara, Turkey.

mantle by flow patterns which reflect the convergence of major plates. If so, seismic velocities in both the upper crust and upper mantle should be anisotropic in their elastic properties (Crampin 1984; Nataf, Nakanishi & Anderson 1986). As part of the present study we attempt to determine whether or not anisotropy in this region can be resolved using seismic surface waves. We will attempt to observe two types of anisotropy: (1) that which produces azimuthal variations of surface-wave group velocities (azimuthal anisotropy) and (2) that which makes it impossible to explain both Rayleigh and Love wave group velocities with a single isotropic model (polarization anisotropy). For the latter case we will invert Rayleigh and Love wave data separately, as well as simultaneously, to see if polarization anisotropy is required. Even though this approach is not strictly valid (Crampin 1970; Mitchell 1984), it will provide an indication of the severity of any polarization anisotropy which might be present.

Pertinent plate tectonic information

The tectonics of the Turkish subplate and surrounding regions is very complex (see Fig. 1) and has been discussed in several studies, some of which are cited in the previous section. Two aspects of the tectonics of this region are pertinent to the present study. The first area of interest is the difference of tectonic regimes in eastern and western Turkey. Eastern Turkey and the Black Sea subplate are sandwiched between the Eurasian plate and the northward moving Arabian plate. By contrast, western Turkey lies adjacent to the SW moving Aegean plate and is a region of N–S extension. It will be interesting to determine whether or not the structure of the crust and upper mantle differs for these regions.

The second area of interest is the position of the Hellenic and Cyprean arcs, the boundaries between the African plate and Aegean plate and Turkish plate, respectively. Since the results of surface-wave studies are least ambiguous when paths are restricted to laterally homogeneous regions, it is advantageous for our study if those boundaries are situated such that the portions of the path which traverse oceanic regions are minimized. The most recent work addressing this issue (e.g. Rotstein & Kafka 1982; Rotstein & Ben-Avraham 1986; Jackson & McKenzie 1988) place that boundary 100–150 km south of the Turkish coast. Thus little, if any, portions of our surface wavepaths should traverse that boundary. As an extreme example, if we have a total path length of 500 km of which 450 km is characterized by a group velocity of 3.0 km s^{-1} and 50 km is characterized by a typical oceanic group velocity of 3.8 k s^{-1}, then the average group velocity would be about 3.06 km s^{-1} or an increase of 2 per cent. Actual portions of oceanic paths should be much smaller than 50 km and should not occur at all for most paths, thus surface-wave velocities along paths from earthquakes on the southern coast of Turkey should therefore not be strongly affected by the presence of oceanic crust. In addition, since the paths are nearly perpendicular to the coast line, there should be

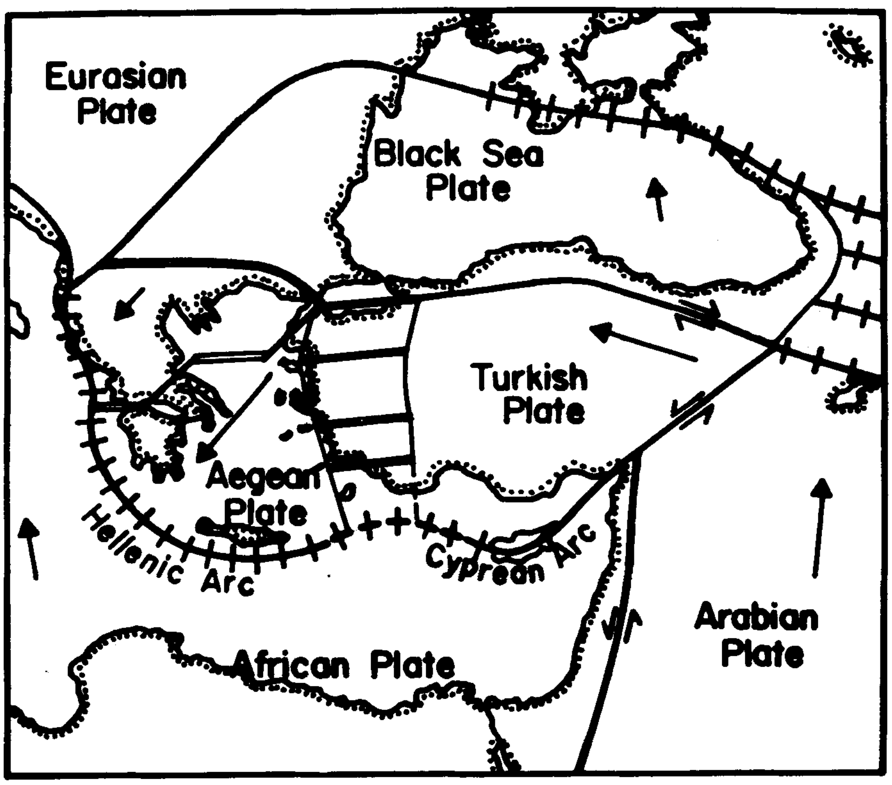

Figure 1. Schematic of plate configuration and movement in the eastern Mediterranean (adapted from McKenzie 1972 and Rotstein & Kafka 1982). Double lines denote plate boundaries across which extension is occurring, single lines indicate transform faults and lines crossed by dashes at right angles denote boundaries across which subduction is taking place. The dashed line indicates uncertain location of boundary. Arrows indicate direction of plate motion relative to Eurasia.

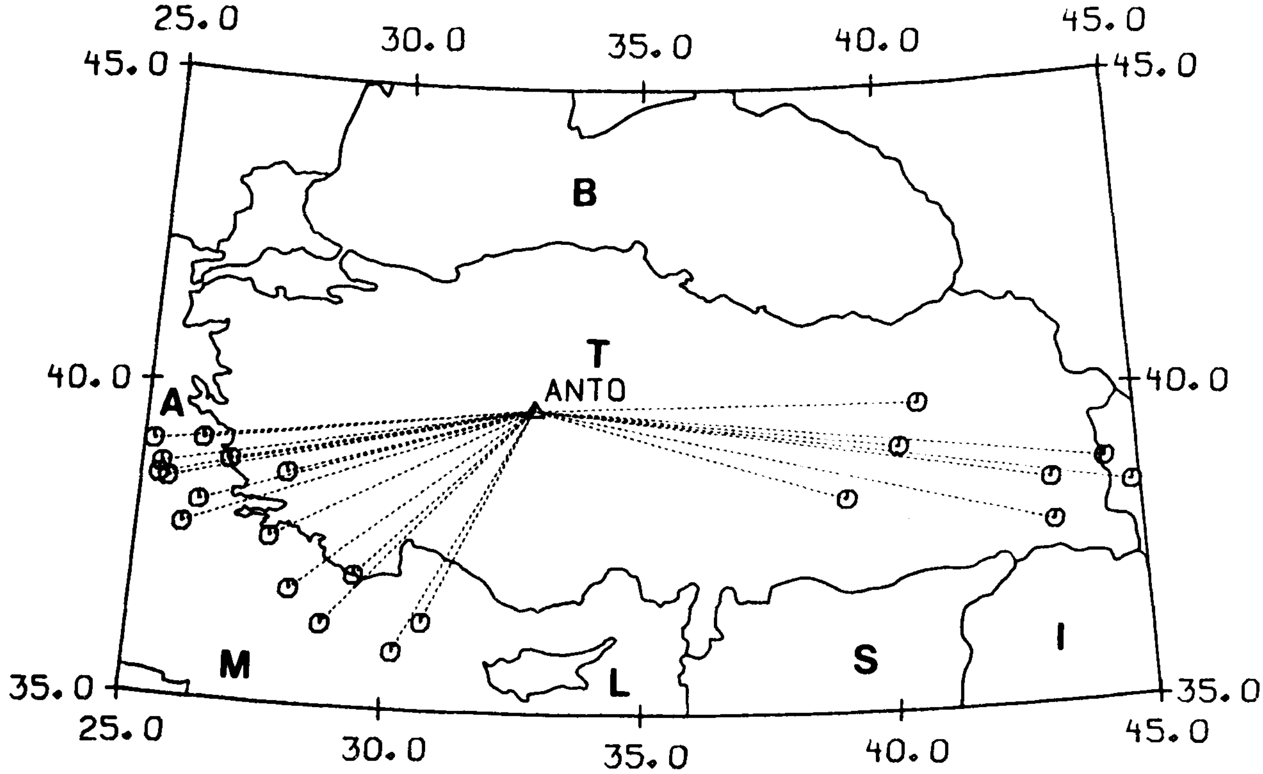

Figure 2. Map showing single-station paths in Turkey. The triangle denotes the seismograph station ANTO and the circles denote earthquake sources. (B, Black Sea; A, Aegean Sea; M, Mediterranean Sea; L, Levantine basin; S, Syria; I, Iraq; T, Turkey.)

no strong adverse effects due to lateral refraction of Rayleigh waves.

DATA

Since the objective of this study is to investigate large-scale varaitions of velocity structure, Turkey is divided into two provinces, eastern Turkey and western Turkey. Paths to the east of the SRO station ANTO lie in the eastern province and paths to the west of ANTO lie in the western province (Fig. 2 and Table 1). We have obtained group velocities for both regions, within each of which it is assumed that elastic properties of the crust and upper mantle are relatively uniform. The pre-Miocene geology of the islands in the

Table 1. Events used in the single-station method.

Region	Date	O.T. (hr min sec)	Lat. (deg) N	Long. (deg) E	Depth (km)	m_b	BAZ (deg)	Δ (km)
ET	4 Jan 81	07:19:45.6	38.443	44.842	33	4.7	95.	1053.
ET	13 Apr 81	19:41:39.9	39.917	40.623	10	4.5	87.	670.
ET	1 Jan 83	23:06:18.5	39.242	40.203	10	4.6	94.	641.
ET	10 Mar 83	05:02:17.2	38.427	39.109	10	4.3	104.	569.
ET	26 Mar 83	10:51:47.3	38.863	44.333	33	4.5	93.	1001.
ET	3 Dec 84	07:38:06.5	37.916	43.240	10	4.8	100.	932.
ET	8 Dec 84	03:19:09.3	38.595	43.227	10	4.7	96.	912.
WT	25 Nov 80	02:31:02.3	38.489	25.519	10	4.6	259.	647.
WT	29 Nov 80	20:03:11.1	38.529	25.341	10	4.6	259.	660.
WT	21 Dec 80	16:28:32.1	39.055	25.173	10	4.5	265.	662.
WT	13 Jan 81	20:22:44.7	38.714	25.366	10	4.2	261.	653.
WT	11 Apr 81	19:21:19.9	38.160	26.167	10	4.1	254.	604.
WT	3 May 81	19:54:43.8	36.412	30.701	59	4.1	206.	425.
WT	11 May 81	19:15:25.3	36.841	28.084	27	4.7	232.	531.
WT	27 Nov 81	13:30:27.9	35.920	30.160	10	4.6	209.	496.
WT	24 Mar 83	10:55:56.9	37.123	29.342	27	4.5	226.	428.
WT	11 Sep 85	11:08:28.9	36.314	28.739	38	4.2	223.	531.
WT	4 Oct 85	13:36:06.9	39.149	26.151	15	4.0	264.	577.
WT	17 Oct 85	19:15:24.9	38.712	27.890	10	4.1	255.	442.
WT	20 Oct 85	07:52:36.2	37.779	25.891	33	4.7	251.	642.
WT	24 Nov 85	01:19:37.6	37.663	27.626	12	4.5	243	511.
WT	23 Dec 85	20:08:59.4	38.854	26.725	33	4.6	260.	535.

ET: Eastern Turkey
ET: Western Turkey

Aegean sea resembles that of Turkey (McKenzie 1978). Thus, since the Aegean region is continental, we combined data from earthquakes in western Turkey and the Mediterranean.

Long-period surface waves at the ANTO station were well recorded at periods between 8 and 50 s for several earthquakes. These are listed in Table 1. An example for the event of 1983 March 26 appears in Fig. 3.

The group velocities of this study were obtained using the multiple-filter method (Dziewonski, Bloch & Landisman 1969). Spectral amplitudes associated with the fundamental mode can be separated from higher modes; thus fundamental-mode group-velocity values can be obtained which are not contaminated by higher-mode interference. Single-station group-velocity measurements are affected by the change of initial phase with frequency; however, this effect may be neglected if epicentral distances are sufficiently large (Kanamori & Abe 1968). Calculated values for this change were found to be inconsequential for the present study so the effect of initial phase was neglected.

Group velocities of fundamental-mode Rayleigh and Love waves were obtained for eastern Turkey (Figs 4a and b) and western Turkey (Figs 4c and d). The means and standard deviations of those velocities, which were used to invert for velocity structure, are given in Table 2.

The uncertaintites to be expected in surface-wave travel times have been discussed by several authors (e.g. Forsyth 1975; Yu & Mitchell 1979). Those time uncertainties which are pertinent to the present study are almost entirely due to uncertainties in origin time and source location. We conservatively estimate that the rms error arising from those effects is 5 s. For an epicentral distance of 650 km (the average path length for this study), this would correspond to a mislocation of about 15 km. Since numerous stations are situated throughout Europe, the Middle East, and Africa, locations should be better than that. Forsyth (1975) also estimates an rms error of 5 s for surface wavepaths in the Pacific, but his error estimate also includes the effects of source finiteness and digitizing error. Those errors can be assumed to be very small in the present study because we use small events ($m_b \leq 4.8$) and digital data. In addition to random errors produced by the above effects, systematic errors may occur. These could be caused by interference with other phases, lateral refraction, or incomplete separation of modes. It is difficult to assess the extent of these effects, but we have estimated that rms errors in group-velocity travel times are about 3.5–4.0 s for Rayleigh waves and 3.0–3.5 s for Love waves. If we add these values to the value of 5.0 discussed above, then for the average path length of this study (about 650 km) and group velocities between 2.7 and 3.3 km s^{-1}, these errors for Rayleigh waves are between 0.10 and 0.14 km s^{-1}. For Love data using group velocities between 2.9 and 3.9 km s^{-1}, they are between 0.11 and 0.21 km s^{-1}. The standard deviations in Figs 6 and 9 are comparable to these values except for the case of Love waves in eastern Turkey. The scatter in the data which produces those large values is evident in Fig. 4(d). Since Love waves are more adversly affected by lateral changes in structure than are Rayleigh waves, those larger errors may suggest that crustal structure in eastern Turkey is more complex than it is in western Turkey and we have underestimated that complexity when estimating rms errors. Alternatively, they may be produced by azimuthal anisotropy, as discussed in a later section.

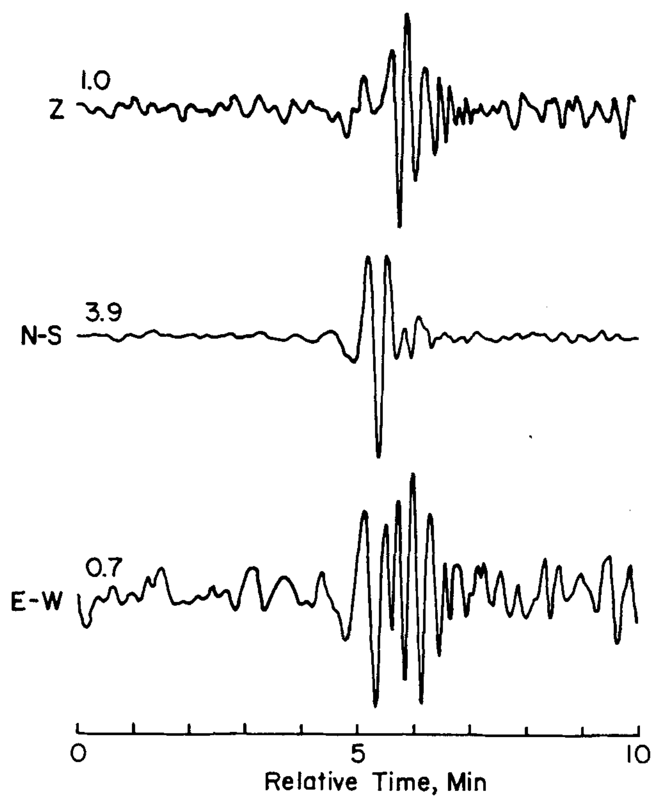

Figure 3. Long-period seismograms recorded on vertical, N–S, and E–W instruments at ANTO for the earthquake of March 26 1983. Numbers by each seismogram indicate maximum amplitudes relative to that of the vertical component. The epicentral distance for this event is 1001 km.

MODELS OBTAINED FROM INVERSION

To obtain models for Turkey, we used inversion theory, as first proposed by Backus & Gilbert (1970). In the present study we used an interactive program developed by Russell *et al.* (1984). That program inverts observed group velocities for plane-layered shear-velocity structures, and uses singular value decomposition (Lawson & Hanson 1974) in stochastic or differential form (Russell 1987).

Our inversion starts with a half-space as the initial model (Fig. 5) and uses a non-linear iterative procedure to arrive at a model which satisfies the data. By starting with a half-space our final model is not biased by any assumptions we make concerning the location of velocity discontinuities in the initial model. The feasibility of using a half-space as the initial model was tested by Hwang & Mitchell (1987) using data from the Indian Shield. They used two starting models, one consisting of a half-space and another based on refraction results. The inversion results were essentially the same for both cases. Since we do not have refraction data for Turkey we could not perform similar tests. We followed the same procedure as that used by Hwang & Mitchell (1987), and used a differential inversion method. The differential inversion process minimizes both the magnitude of the error vector between observed and computed

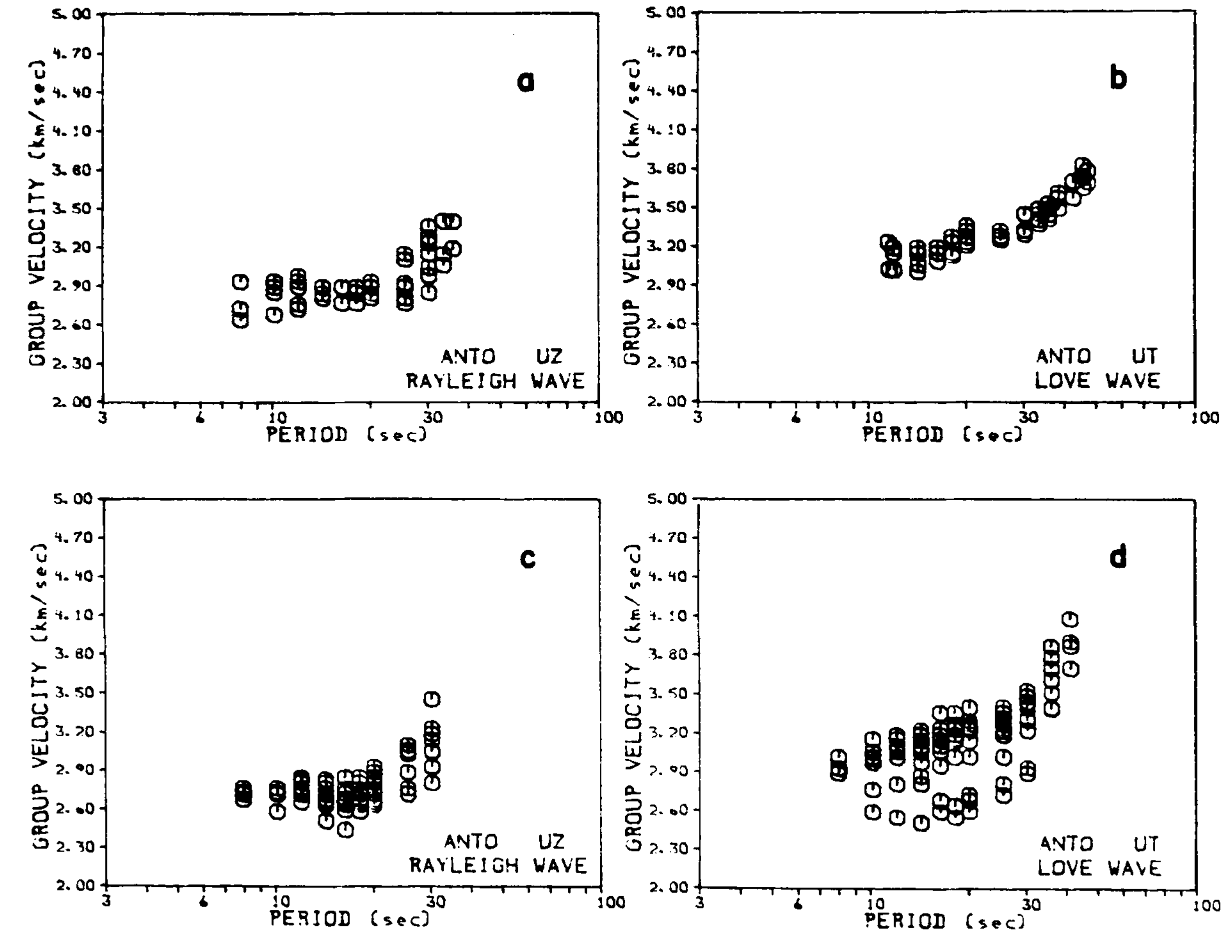

Figure 4. Group velocity data obtained for the earthquakes of Table 1: (a) and (b) for eastern Turkey, (c) and (d) for western Turkey.

velocities and differences between adjacent layers, thereby minimizing large velocity changes between adjacent layers. Our inversion results are restricted to shear velocities because that parameter has a far greater effect on surface-wave velocities than does compressional-wave velocity or density throughout most of the model. The latter parameters could have some effect at shallow depths, but at those depths Poisson's ratio can be assumed to be known reasonably well, thus constraining compressional velocities while empirical relations can constrain density values. Poisson's ratio was assumed to be 0.25 in the crust and 0.27 in the upper mantle for all inversions, and densities were

Table 2. Means and standard deviations of group velocities in Turkey (km/s) (fundamental mode).

Period (sec)	Eastern Turkey U_R	Eastern Turkey U_L	Western Turkey U_R	Western Turkey U_L
8.0	2.752±0.127		2.737±0.034	2.942±0.054
10.0	2.857±0.107		2.732±0.062	2.954±0.184
11.0		3.122±0.149		
12.0	2.869±0.103	3.166±0.088	2.765±0.057	3.013±0.192
14.0	2.867±0.037	3.107±0.075	2.706±0.089	3.028±0.212
16.0	2.867±0.051	3.148±0.043	2.681±0.101	3.066±0.223
18.0	2.852±0.046	3.208 ±0.070	2.703±0.073	3.112±0.258
20.0	2.864±0.049	3.275±0.062	2.756±0.095	3.097±0.263
25.0	2.996±0.165	3.294±0.036	2.900±0.131	3.186±0.210
30.0	3.123±0.179	3.359±0.076	3.108±0.197	3.295±0.222
33.0	3.202±0.176	3.434±0.052		
36.0	3.295±0.151	3.477±0.052		3.606±0.185
38.0		3.537±0.063		
41.0				3.884±0.156
42.0		3.609±0.073		
45.0		3.694±0.063		
47.0		3.734±0.064		

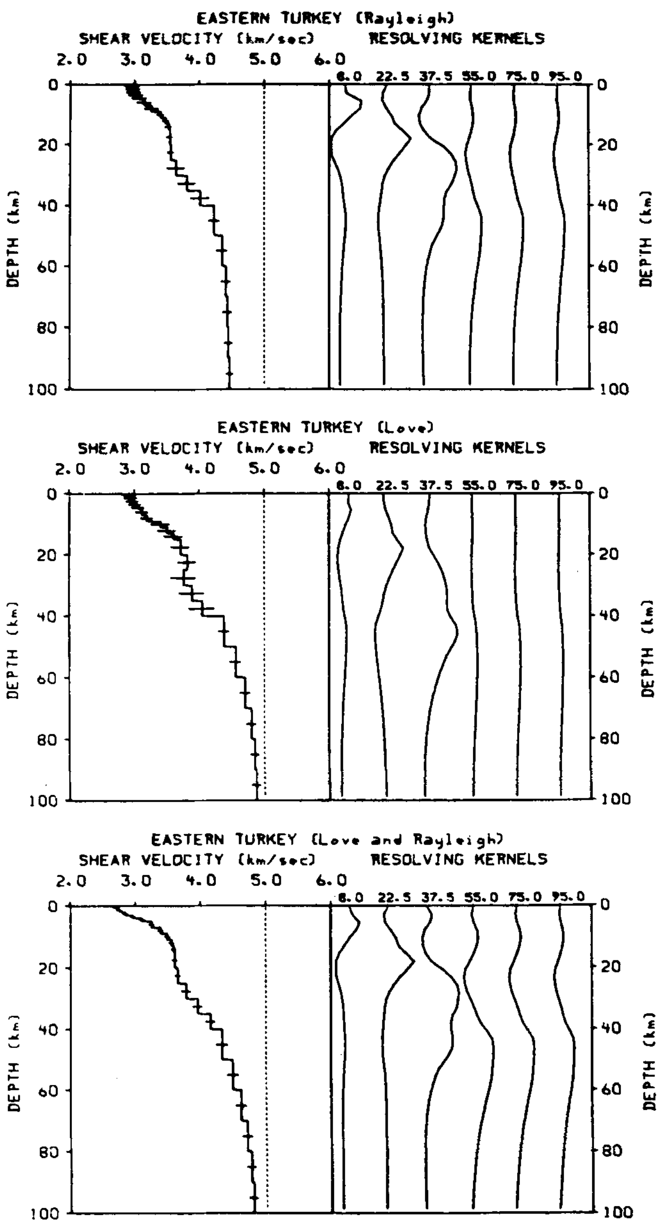

Figure 5. Shear-wave models (solid line) for eastern Turkey obtained from inversions of Rayleigh wave data, Love wave data, and combined Rayleigh and Love wave data. The dashed lines indicate the initial half-space model. Resolving kernels corresponding to several depths between 8 and 95 km are also shown.

calculated using known relations between density and compressional-wave velocity in the crust (Talwani, Sutton & Worzel 1959) and mantle (Birch 1964). If the value for Poisson's ratio in the crust is off by 8 per cent, and the compressional wave velocity is 6.0 km s^{-1}, then shear wave velocities will be off by only about 3 per cent.

Our procedure for obtaining a velocity model includes the determination of the necessity of discontinuities or rapid gradients and can be summarized as follows. Dispersion data are inverted, using a half-space starting model, and a model is obtained through a non-linear iterative process in which velocity partial derivatives are recomputed for each iteration. If successful convergence has been achieved, theoretical group velocities should agree with observed values within the data uncertainties. We also obtain resolving lengths and values for model parameter uncertainties at all depths. The resolving lengths refer to sensitivity to only shear-wave velocities for the inversions, thus if our compressional-wave velocities and densities are not reasonably close to true values, resolution may be poorer than that shown in Figs 5 and 8 at shallow depths. A trade-off exists between model uncertainties and resolution and we can set a trade-off parameter so as to achieve smaller model undertainties at the expense of resolution, and vice versa. We have chosen the trade-off parameter so that models have the best possible resolution within the constraint that they be realistic, i.e. they do not contain large fluctuations in velocity. Steep velocity gradients often appear in the resulting model. Because of the limited resolving power of surface waves, these gradients may actually correspond to velocity discontinuities.

Eastern Turkey

The dispersion data in Table 2 were used to obtain a velocity model for eastern Turkey from Rayleigh waves. The resulting model is plotted in Fig. 5 along with its resolving kernels. The initial model was a half-space having a shear-wave velocity of 5 km s^{-1}. Rapid velocity gradients occur at depths between 5 and 10 km, and between 30 and 40 km. The crust–mantle transition in this region may occur at about 40 km where there is an increase in velocity to 4.2 km s^{-1}. Note that since the resolution for the lower crust and upper mantle is relatively poor, no detail could be resolved for this region. This poor resolution results in small model uncertainties in our velocity model at larger depths (Fig. 5). The seismic velocities for this model are listed in Table 3 together with depths, thicknesses, and densities.

We also inverted the Love wave data of Table 2 to obtain a second velocity model for eastern Turkey (Fig. 5 and Table 3 (L)). A rapid gradient occurs at depths between 5 and 15 km. At shallow depths velocities are similar to those obtained from the inversion of Rayleigh waves, but at greater depths velocities are greater for the love wave inversion than the Rayleigh wave inversion. Another rapid gradient occurs at a depth of about 40 km.

Love and Rayleigh waves were inverted simultaneously to obtain the model of Fig. 5 and Table 3 (L and R). Rapid gradients occur at depths between 0 and 5 km and at depths between 30 and 40 km. The observed and theoretical surface wave velocities are compared in Fig. 6. In this figure the solid lines show the results from combined inversions. Note that the calculated Love wave velocities for the model obtained from the simultaneous inversion are very similar to those obtained from the inversion of Love wave data alone, even though these models are somewhat different. This occurs because of the relatively poor resolving power of the Love wave data compared with that of Rayleigh waves.

The three derived velocity models are compared in Fig. 7. The model obtained from the inversion of Rayleigh waves is significantly slower than that obtained from Love waves, a result sometimes taken to imply polarization anisotropy of upper mantle material (e.g. McEvilly 1964). The combined inversion, however, explains the data equally well; therefore polarization anisotropy does not seem to be required to

Table 3. Velocity models for eastern Turkey.

H (km)	T (km)	α (km/s)			β (km/s)			ρ (g/cm³)		
		R	L	L&R	R	L	L&R	R	L	L&R
1.0	1.0	5.15	5.09	4.69	2.98	2.94	2.71	2.53	2.52	2.43
2.0	1.0	5.16	5.11	4.78	2.98	2.95	2.76	2.53	2.52	2.45
3.0	1.0	5.18	5.16	4.94	2.99	2.98	2.85	2.54	2.53	2.49
4.0	1.0	5.24	5.22	5.15	3.02	3.01	2.97	2.55	2.54	2.53
5.0	1.0	5.33	5.31	5.38	3.08	3.06	3.11	2.57	2.56	2.58
7.0	2.0	5.47	5.41	5.64	3.16	3.12	3.25	2.59	2.58	2.63
9.0	2.0	5.66	5.56	5.87	3.27	3.20	3.39	2.63	2.61	2.67
11.0	2.0	5.90	5.91	6.06	3.40	3.41	3.50	2.68	2.68	2.72
13.0	2.0	6.04	6.08	6.17	3.49	3.51	3.56	2.71	2.72	2.75
15.0	2.0	6.12	6.26	6.23	3.53	3.61	3.60	2.73	2.78	2.77
20.0	5.0	6.14	6.44	6.25	3.55	3.72	3.61	2.74	2.83	2.78
25.0	5.0	6.18	6.62	6.33	3.57	3.82	3.65	2.75	2.88	2.80
30.0	5.0	6.32	6.52	6.55	3.65	3.76	3.78	2.80	2.85	2.86
35.0	5.0	6.61	6.74	6.86	3.82	3.89	3.96	2.88	2.91	2.94
40.0	5.0	6.95	7.01	7.20	4.02	4.05	4.15	2.97	2.98	3.04
50.0	10.0	7.54	7.81	7.72	4.23	4.38	4.33	3.15	3.24	3.22
60.0	10.0	7.76	8.12	8.01	4.35	4.56	4.49	3.23	3.35	3.31
70.0	10.0	7.86	8.38	8.23	4.41	4.70	4.62	3.26	3.45	3.39
80.0	10.0	7.91	8.56	8.40	4.44	4.80	4.71	3.28	3.51	3.45
90.0	10.0	7.93	8.65	8.51	4.45	4.86	4.77	3.29	3.54	3.49
100.0	10.0	7.96	8.69	8.56	4.47	4.88	4.81	3.30	3.55	3.51
	∞	8.01	8.69	8.58	4.50	4.88	4.81	3.31	3.55	3.52

explain both datasets. If we take $4.2\,\mathrm{km\,s^{-1}}$ to correspond to upper mantle shear velocities, then the total crustal thickness is about 40 km.

The three models of Fig. 7 differ from one another through portions of their depth range by more than the model uncertainties in Fig. 5. Two factors may cause these differences. Polarization anisotropy may be present throughout portions of the model. Such anisotropy could cause the models resulting from separate inversions of Love and Rayleigh waves to differ considerably. A simultaneous

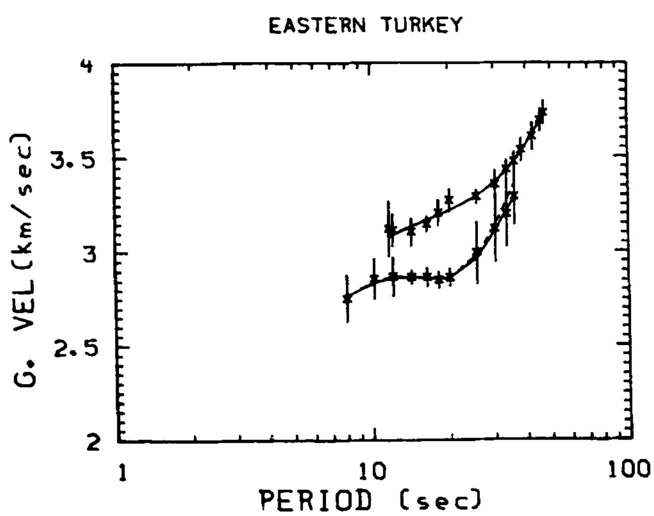

Figure 6. The theoretial dispersion values predicted by the models compared with observed Rayleigh and Love dispersion values in eastern Turkey. The solid lines are from the separate inversions and the dashed lines are from the combined inversion. Vertical lines indicate standard deviations for the observed data. The dashed line is overlain by the solid line over much of the period ranges of both Rayleigh and Love waves.

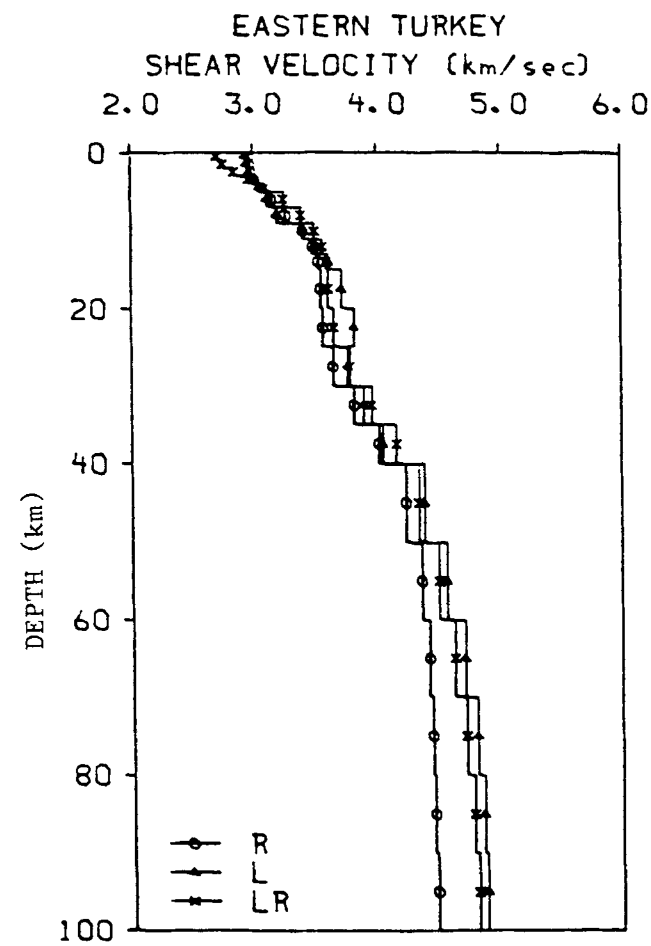

Figure 7. Comparison of models for eastern Turkey obtained by inverting group velocities of fundamental-mode Love waves (L), Rayleigh waves (R) and combined Love and Rayleigh waves (LR).

inversion of the data, erroneously assuming an isotropic model, may produce unrealistically high or low values through some portions of the models in an attempt to fit both sets of data. This occurs because the maximum sensitivities of Rayleigh and Love waves to elastic properties, for a given period, generally occurs through different depth ranges. The resulting models may include layers which are unrealistically high or low or may include more modest fluctuations which could be interpreted as real features (Mitchell 1984). Since the errors thus produced are systematic, rather than random, the error bars in the model may not overlap. This is particularly true at depths where resolution is very poor, as it is for Love waves at depths greater than about 50 km. For cases such as that the error bars can be misleading since they represent uncertainty of a broad average of model properties around the specified depth. The same effect could occur if systematic errors, not reflected in the data uncertainties, occur in the group velocities. Some fluctuations in our group velocity values, such as that for the Love wave data near 20 s in Fig. 6 may reflect such systematic errors.

The P_n velocity which corresponds to the shear velocity obtained from Rayleigh waves below a depth of 40 km, assuming a Poisson's rato value of 0.27, is 7.54 km s^{-1} (Table 3). This is considerably lower than values obtained in other continental regions and in other studies of Turkey. Canitez & Toksoz (1980), using travel times and station residuals of *P*-waves, found a P_n velocity in eastern and northern Turkey of 7.9 km s^{-1}. These results therefore suggest that Poisson's ratio in the uppermost mantle is larger than the value of 0.27 which we assumed. In order to satisfy our Rayleigh wave data, as well as that of Canitez & Toksoz (1980), the Poisson's ratio would need to be 0.30. In order to satisy the results of our combined inversion of Rayleigh and Love wave data and the data of Canitez & Toksoz (1980) it would have to be 0.29.

None of the results of inversion require a low-velocity zone in the upper mantle. This result does not necessarily imply that no low-velocity zone exists there; one may exist but may be either too deep or too minor to be resolved by our data.

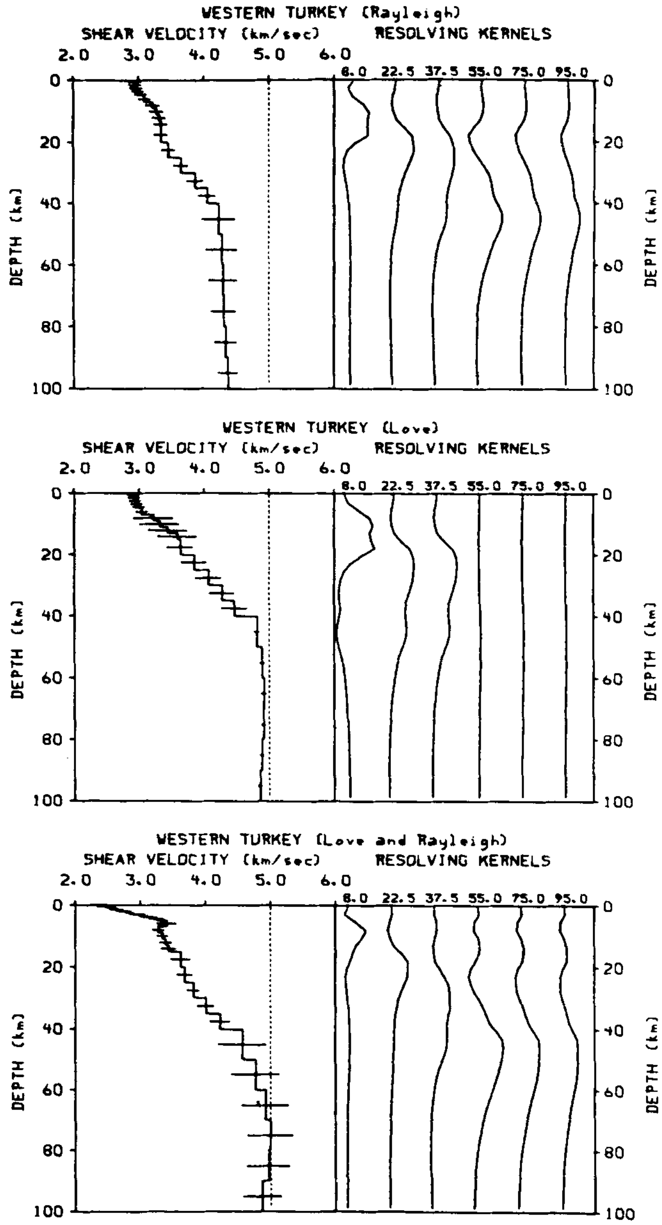

Figure 8. Shear-models (solid line) for western Turkey obtained from inversions of Rayleigh wave data, Love wave data, and combined Rayleigh and Love wave data. The dashed lines indicate the initial half-space model. Resolving kernels corresponding to several depths between 8 and 95 km are also shown.

Western Turkey

The Rayleigh wave dispersion data in Table 2, along paths to the west of ANTO, were used to obtain a velocity model for western Turkey. The resulting model is plotted in Fig. 8 along with its resolving kernels. The initial model was a half-space having a shear wave velocity of 5 km s^{-1}. The crust–mantle transition for this model in western Turkey is also gradational just as that for eastern Turkey. The widths of the resolving kernels at these depths, however, indicate that detail cannot be resolved in this region and a sharp discontinuity could occur there. The velocities are listed in Table 4 (R) together with depths, thicknesses and densities.

A velocity model for western Turkey was also obtained using the Love wave data of Table 2 (Fig. 8 and Table 4 (L)). Rapid gradients occur between near-surface depths and 17 km, and between about 20 and 40 km, with an abrupt increase in velocity at 40 km. The velocities are listed in Table 4 and are faster than those obtained using Rayleigh waves at most depths in the crust and upper mantle.

A simultaneous inversion of Love and Rayleigh waves leads to the model in Fig. 8 and Table 4 (L and R). The observed and theoretical surface wave velocities are compared in Fig. 9. Except for one Love wave data point at a period of 40 s, it adequately explains all of the Rayleigh and Love wave velocities (Fig. 9). Our inability to explain that value may be due to an underestimation of the error there since only four data points were used or because low values through the period range 10–30 s bias the mean group velocities in that region making it difficult to invert all of the data to obtain a realistic model. Those low values are discussed in a later section in the context of possible azimuthal anisotropy in western Turkey. The model of Fig.

Table 4. Velocity models for western Turkey.

H (km)	T (km)	α (km/s)			β (km/s)			ρ (g/cm^3)		
		R	L	L&R	R	L	L&R	R	L	L&R
1.0	1.0	5.11	5.06	4.30	2.95	2.92	2.48	2.52	2.51	2.36
2.0	1.0	5.12	5.07	4.57	2.96	2.93	2.64	2.52	2.51	2.41
3.0	1.0	5.14	5.10	4.94	2.97	2.94	2.85	2.53	2.52	2.49
4.0	1.0	5.19	5.14	5.31	2.99	2.97	3.06	2.54	2.53	2.56
5.0	1.0	5.26	5.20	5.64	3.04	3.00	3.25	2.55	2.54	2.63
7.0	2.0	5.36	5.28	5.91	3.10	3.05	3.41	2.57	2.56	2.68
9.0	2.0	5.57	5.59	5.69	3.22	3.23	3.29	2.61	2.62	2.64
11.0	2.0	5.68	5.75	5.80	3.28	3.32	3.35	2.64	2.65	2.66
13.0	2.0	5.75	5.97	5.89	3.32	3.45	3.40	2.65	2.69	2.68
15.0	2.0	5.81	6.23	5.96	3.35	3.60	3.44	2.66	2.77	2.69
20.0	5.0	5.81	6.30	6.27	3.35	3.64	3.62	2.66	2.79	2.78
25.0	5.0	6.00	6.67	6.38	3.46	3.85	3.69	2.70	2.89	2.82
30.0	5.0	6.34	7.06	6.62	3.66	4.07	3.82	2.80	3.00	2.88
35.0	5.0	6.72	7.42	6.95	3.88	4.28	4.01	2.91	3.11	2.97
40.0	5.0	7.04	7.74	7.32	4.07	4.47	4.23	2.99	3.22	3.08
50.0	10.0	7.55	8.58	8.15	4.24	4.81	4.57	3.16	3.52	3.36
60.0	10.0	7.64	8.72	8.50	4.29	4.89	4.77	3.19	3.56	3.49
70.0	10.0	7.66	8.77	8.78	4.30	4.92	4.93	3.20	3.58	3.58
80.0	10.0	7.69	8.76	8.91	4.31	4.91	5.00	3.20	3.58	3.63
90.0	10.0	7.73	8.71	8.86	4.34	4.89	4.97	3.22	3.56	3.61
100.0	10.0	7.80	8.67	8.68	4.38	4.86	4.87	3.24	3.55	3.55
	∞	7.88	8.62	8.43	4.42	4.84	4.73	3.27	3.53	3.46

8 includes gradients between the surface and 5 km, and between 25 and 40 km, and a possible discontinuity occurs at 40 km. A slight low-velocity zone occurs at depths between 7 and 13 km, but the resolving kernels indicate that it is not a resolvable feature.

The three derived velocity models for western Turkey are compared in Fig. 10. The differences between the models may be produced by the same factors discussed in the section on eastern Turkey. A discontinuity may occur at a depth of 40 km where velocities increase to values typical of upper mantle shear velocities. The model obtained from the inversion of Rayleigh waves, like eastern Turkey, is slower

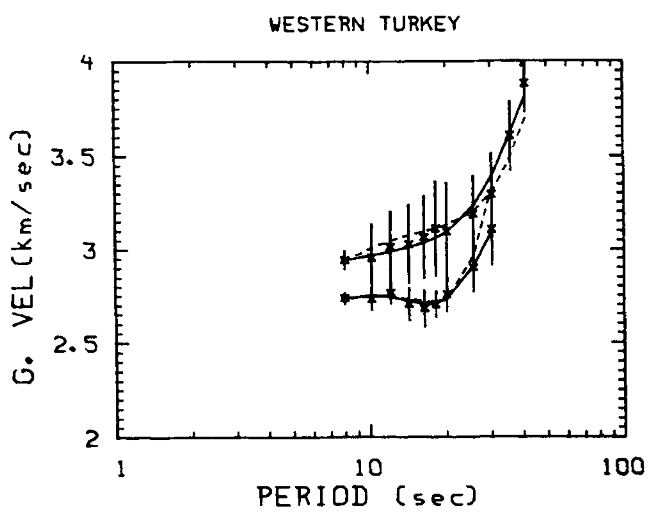

Figure 9. The theoretical dispersion values predicted by the models compared with observed Rayleigh and Love dispersion values in western Turkey. The solid lines are from the separate inversions and the dashed lines are from the combined inversion. Vertical lines indicate standard deviations for the observed data.

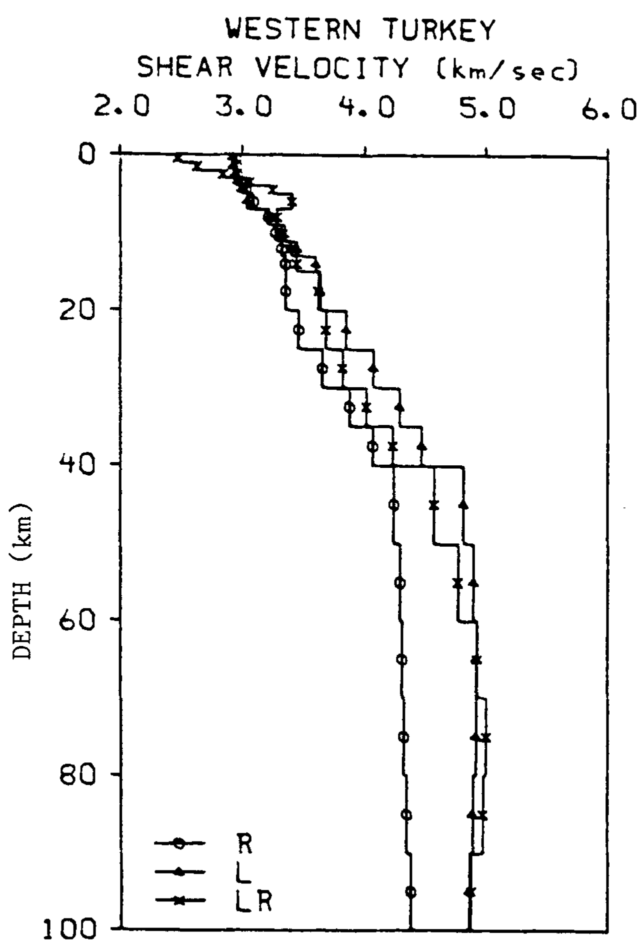

Figure 10. Comparisons of models for western Turkey obtained by inverting group velocities of fundamental Love waves (L), Rayleigh waves (R) and combined Love and Rayleigh waves (LR).

than that obtained from the inversion of Love waves, suggesting the possibility of polarization anisotropy, but the model resulting from combined inversion also explains the data adequately. The different models suggested by the individual inversions of Love and Rayleigh waves may therefore only be an artifact of poor resolution and may not indicate polarization anisotropy. The differences between the three models of Fig. 10 are greater than the model uncertainties, as they were for eastern Turkey. This again could be due to anisotropy or to systematic errors in the observations which have not been accounted for. The resolution for Love waves at depths greater than 50 km is extremely poor, thus, as stated earlier, model uncertainties at those depths may be misleading. Additional high-resolution Rayleigh and Love wave data will be required to conclusively demonstrate that polarization anisotropy is necessary in order to produce the differences in the models obtained by individual inversions of Rayleigh and Love waves.

Regional comparison

The two models, derived using combined Love and Rayleigh waves, for both regions of Turkey appear in Fig. 11. The models for eastern Turkey and western Turkey are similar

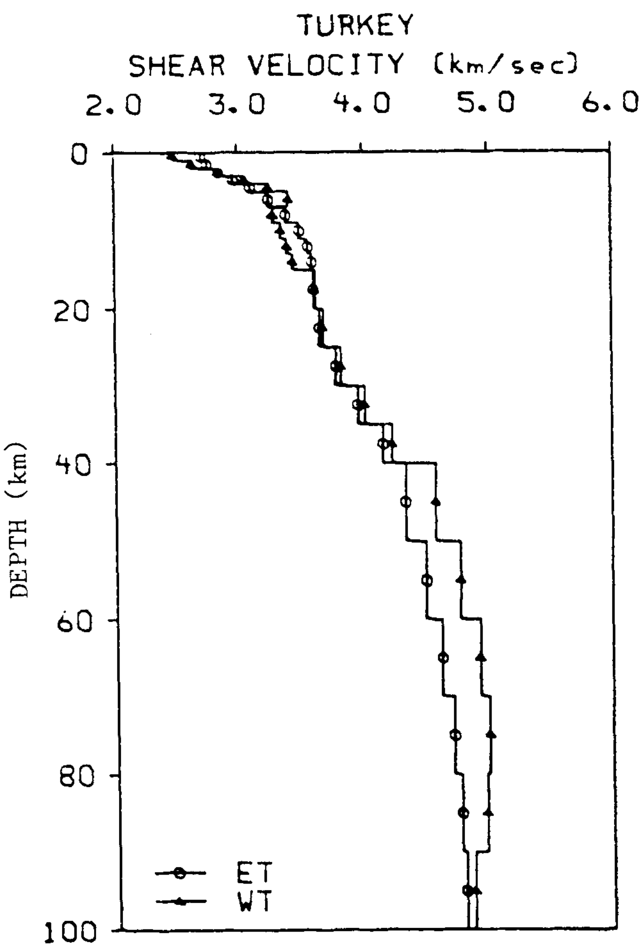

Figure 11. Comparison of models for eastern and western Turkey as obtained from a combined inversion of Love and Rayleigh wave data.

to one another throughout the uppermost crust and lower crust. Velocities for eastern Turkey are, however, about $0.15\ \mathrm{km\ s^{-1}}$ faster than those for western Turkey through the depth range 6–15 km. The resolving lengths and uncertainties in Figs 5 and 8 indicate that this difference is resolvable. At upper mantle depths shear velocities for western Turkey are about $0.3\ \mathrm{km\ s^{-1}}$ faster than those of eastern Turkey. Although resolution is poor for mantle depths, the consistency of this difference over a large depth range indicates that average velocity differences there are likely to be correct. If we take $4.2\ \mathrm{km\ s^{-1}}$ to represent the upper mantle shear velocity, the crust–mantle boundary occurs at a depth of about 40 km in both regions.

Both the crustal velocities and upper mantle velocities obtained for Turkey are lower than those obtained throughout most of Europe, but are similar to those obtained in some regions in and near the Mediterranean. We obtained values less than $3.0\ \mathrm{km\ s^{-1}}$ for the uppermost crust, whereas values of 3.0–$3.5\ \mathrm{km\ s^{-1}}$ have been obtained by Knopoff, Mueller & Pilant (1966) in the Alps, values of 3.5–$3.6\ \mathrm{km\ s^{-1}}$ have been obtained by Der & Landisman (1972) in Scandinavia and values of 3.1–$3.5\ \mathrm{km\ s^{-1}}$ have been obtained by Dost (1987) in the west European platform. Our upper mantle values of 4.2–$4.3\ \mathrm{km\ s^{-1}}$ are also lower than upper mantle values throughout most of Europe where, with few exceptions, they are greater than $4.5\ \mathrm{km\ s^{-1}}$ (Panza, Mueller & Calcagnile 1980). Our upper mantle values are, however, similar to values reported by Panze *et al.* (1980) for the western Mediterranean and a small portion of SW Germany.

Possible crustal anisotropy in western Turkey

The Rayleigh and Love waves recorded in western Turkey display greater scatter than those recorded in eastern Turkey and were obtained over a broader range of azimuths (Figs 4c, d and Table 2). There is a possibility that these observed variations in group velocity in western Turkey could be produced by azimuthal anisotropy of elastic properties in the crust or upper mantle. The azimuthal variation of observed Rayleigh wave group velocities for all of the earthquakes to the west of ANTO is shown in Fig. 12 and that for Love wave group velocities appears in Fig. 13.

Theoretical calculations of Crampin & Taylor (1971) for models with a horizontal axis of symmetry show that the azimuthal variation of Rayleigh wave velocities will vary as 2Θ with the maximum velocity being in the direction of compressional and vertically polarized shear waves. Love waves display a 4Θ variation and the maximum velocity for Love waves differs from that of Rayleigh waves by 45°. The observed data of Figs 12 and 13 suggest that this relationship between Rayleigh and Love wave velocities may occur in western Turkey. Theoretical values shown by the solid and dashed lines in Figs 12 and 13 were computed for two different anisotropic models of the upper crust overlying an isotropic lower crust and upper mantle. The theortical formulation required for computing surface-wave velocities in generalized anisotropic media was developed by Crampin (1970) and Crampin & Taylor (1971). Crampin (1978, 1981, 1984) and Hudson (1981) calculated the variations of velocity of seismic waves propagating through solids containing aligned cracks.

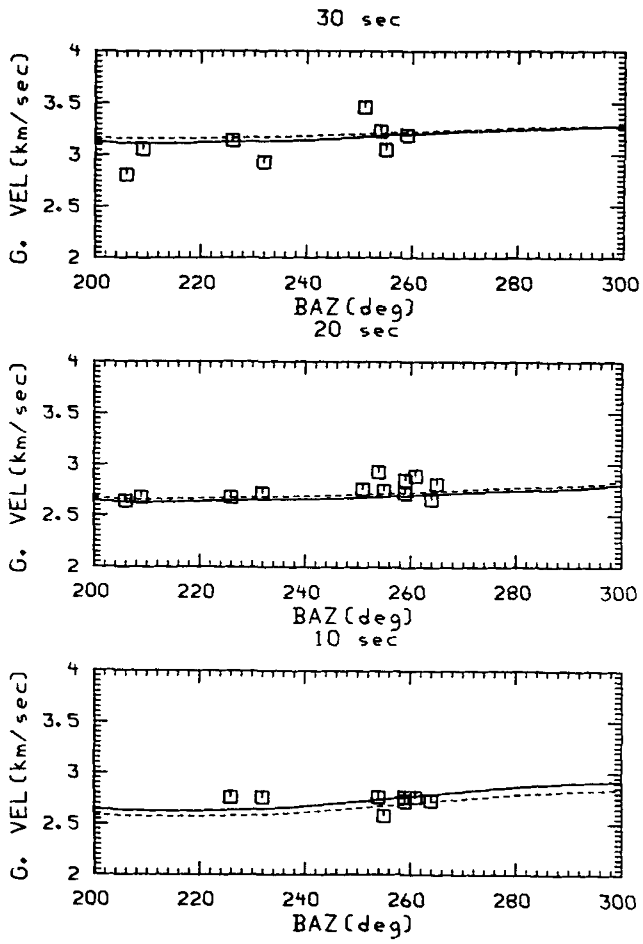

Figure 12. Azimuthal variation of group-velocity data of Rayleigh waves for western Turkey at periods of 10, 20, and 30 s. The symbols denote the observed data. The solid and dashed lines correspond respectively to models A and B.

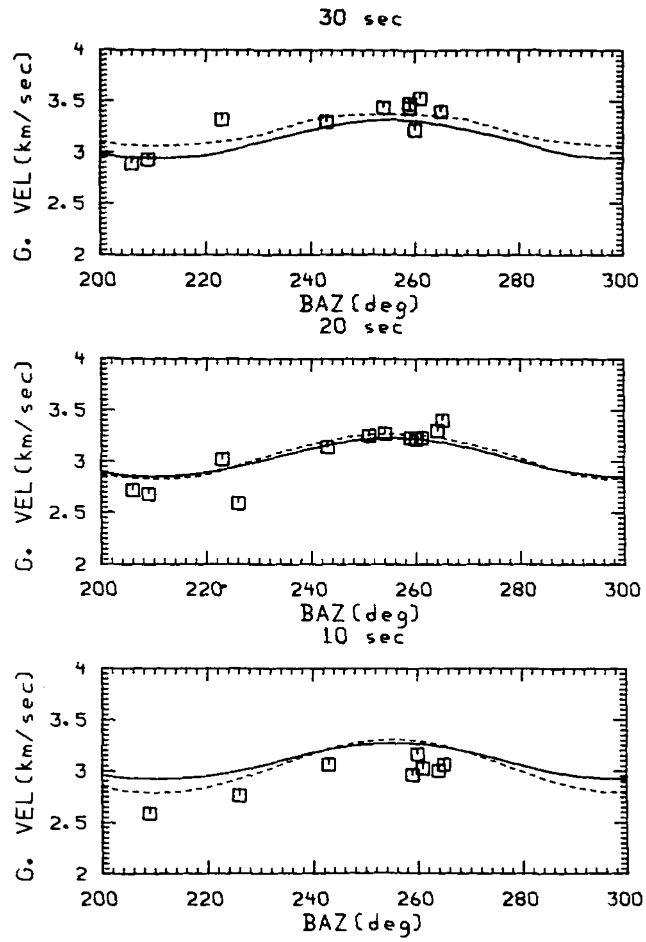

Figure 13. Azimuthal variation of group-velocity data of Love waves for western Turkey at periods of 10, 20, and 30 s. The symbols denote the observed data. The solid and dashed lines correspond respectively to models A and B.

Two anisotropic models were considered in this study. For model A the anisotropic portion of the crust was taken to be between depths of 0 and 20 km and to consist of vertical, water-saturated cracks with the elastic constants of Crampin (1984). These constants appear in Table 5. For model B the three elastic constants which have the greatest effect on generalized waves (Anderson 1961) have been reduced by 10 per cent compared with those of model A (Table 5) and the thickness of the anisotropic crust is taken to be 10 km. The elastic constants for model A correspond to a crust containing vertical cracks with a density of 0.1, each with a radius of 5 m, and an aspect ratio of 0.0001. The reduced values for model B imply either an increase in crack density or an increase in size of the cracks compared with those of model A. For both models, the lower crust and upper mantle velocities are those presented in Table 4 (L and R). These models produce the theoretical group velocities shown by the solid and dashed lines in Figs 12 and 13. If the direction of cracking is N 120° E, the observed azimuthal variation is predicted well; the absolute level is also predicted well except for the case of Rayleigh waves at a period of 10 s. This difference is probably due to the oversimplified model of the upper crust needed to perform the anisotropic computations.

Table 5. Elastic constants for wave propagation through a system of vertical, water-saturated parallel cracks of density 0.1, each having a radius of 5 m and an aspect ratio of 0.0001. Model A is taken from Crampin (1984), and model B is the same model except that C_{2323}, C_{1212}, and C_{1313} are reduced by 10 per cent.

	Model A	Model B
C_{1111}	87.322	87.322
C_{2222}	87.448	87.448
C_{3333}	87.448	87.448
C_{2233}	29.126	29.126
C_{1122}	29.102	29.102
C_{1133}	29.102	29.102
C_{2323}	29.161	26.245
C_{1212}	23.261	20.935
C_{1313}	23.261	20.935

Considering the high temperatures and pressures likely to occur at depths of 20 km in the crust, it is less likely that open cracks would occur there than at shallow depths; thus model B, having a thinner layer of more highly anisotropic material, has also been considered in our calculations. Although model B provides a slightly better fit to our data, the improvement is not sufficiently large to decide between the models. The direction N 120° E predicted by the group-velocity data is within 30° of the directions of lineaments observed on satellite images of the Aegean basin (Foose 1985). The existence of cracks orientated roughly in an E–W direction is also consistent with the interpretation of N–S extension in western Turkey from focal mechanisms studies (McKenzie 1978) and from plate tectonic reconstructions of the area (Dewey & Sengor 1979; Sengor & Yilmaz 1981).

Figure 14 shows the theoretical variation of velocities at all azimuths for both models. This illustrates the 2Θ variation of Rayleigh wave velocities and the 4Θ variations of Love wave velocities in these models. Although it would be beneficial to have group velocity data over a greater range of azimuths, both the form and the relative amplitudes of the observed azimuthal variations are consistent with these calculations. Note that the observed Love wave velocities are larger and their azimuthal variation more rapid than the observed Rayleigh wave variations as predicted by the calculated values of Fig. 14.

The conclusion that azimuthal anisotropy, arising from vertical cracks, may occur in the upper crust is similar to that of Crampin & Booth (1985) who studied shear waves in NW Turkey near the north Anatolian fault. They explained observed splitting of shear waves in terms of fluid-filled crack-induced anisotropy. They also used Crampin's (1984) anisotropic crack model for a 10 km portion of the upper crust. Our results, suggesting either a greater depth extent of cracking or more extensive fracturing over the same depth interval as that of Crampin & Booth (1985), may indicate that greater deformation is occurring in southern Turkey than in northern Turkey.

Although the degree and direction of anisotropy required to explain the surface wave data of this study are consistent with plate tectonic models and geological information, it is also possible that the azimuthal group velocity variations in western Turkey could be explained by regional variations of velocity. However, available geological and geophysical data are more consistent with the interpretation of anisotropy than with interpretation of regional variations in velocity. In addition to arguments above, which appealed to focal mechanisms, lineations, and plate tectonic reconstructions, we can also cite heat flow values inferred from the map compiled by Cermak & Zahradnik (1982). These are higher for western Turkey (90–110 mW m^{-2}) than for SW Turkey (50–90 mW m^{-2}). Since higher heat flow values usually correspond to lower velocities, the opposite of the situation we have observed, these values argue against the likelihood that the higher seismic velocities observed in western Turkey are due to regional variations in crustal structure.

CONCLUSIONS

Our surface wave studies in Turkey lead to the following conclusions:

1. Crustal and upper mantle shear-wave velocities in Turkey obtained in this study are lower than those in most other parts of Europe outside of the Mediterranean region.

2. If the upper mantle shear velocity beneath Turkey is 4.2 km s^{-1}, then Poisson's ratio in the upper mantle may be as high as 0.31.

3. Satisfactory fits to both Rayleigh and Love wave data do not require polarization anisotropy of crustal or mantle elastic properties, but that possibility cannot be excluded.

4. The crust–mantle boundary is not well resolved in either eastern or western Turkey. However, if we take a shear velocity of 4.2 km s^{-1} or greater to define the Moho,

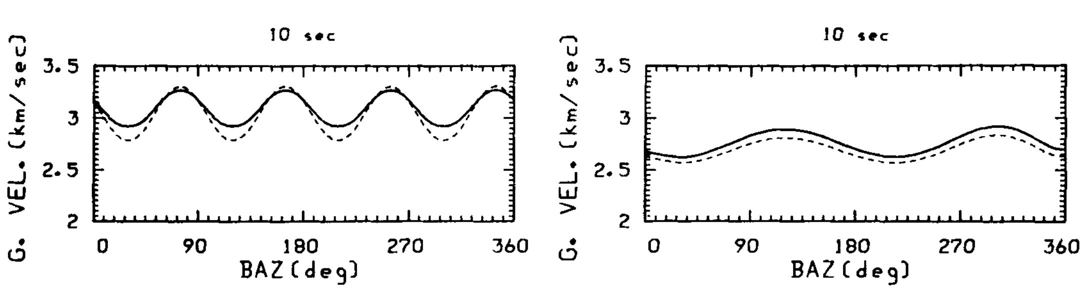

Figure 14. The theoretical azimuthal variation of group-velocity data of Love waves (left) and Rayleigh waves (right) for periods of 10 and 30 s. The solid and dashed lines correspond respectively to models A and B.

then the crustal thickness in all regions is about 40 km. Our models indicate a diffuse velocity increase between mid-crustal depths and Moho in Turkey, but it is possible that more abrupt increases occur but cannot be resolved by the data.

5. Shear velocities are higher in the depth range 6–15 km in eastern Turkey than in westen Turkey.

6. Shear velocities in the upper mantle or eastern Turkey are lower than those of western Turkey.

7. Azimuthal variations of Rayleigh and Love wave group velocities in western Turkey, a region of N–S crustal extension, are consistent with velocities predicted by an anisotropic upper crust in which vertical cracks are orientated in an approximate E–W direction.

ACKNOWLEDGMENTS

Programs used for surface wave analyis were writen by R. B. Herrmann and C. Y. Wang, those for the inversion of surface wave dispersion by D. Russell, and for computing surface-wave dispersion in anisotropic media by S. Crampin and D. B. Taylor. This research was supported by the Division of Earth Sciences, National Science Foundation, under Grant EAR-8804355. O. Y. Mindevalli received partial support from NATO during the period of this research.

REFERENCES

Anderson, D. L., 1961. Elastic wave propagation in layered anisotropic media, *J. geophys. Res.*, **66**, 2953–2963.

Backus, G. & Gilbert, F., 1970. Uniqueness in the inversion of inaccurate gross earth data, *Phil. Trans. R. Soc. A*, **266**, 123–192.

Birch, F., 1964. Density and composition of mantle and core, *J. geophys. Res.*, **69**, 4377–4388.

Canitez, N. & Toksöz, M. N., 1980. Crustal structure beneath Turkey, *Eos Trans. Am. geophys. Un.*, **61**, 290.

Cermak, V. & Zahradnik, J., 1982. Two-dimensional correlation of heat flow and crustal thickness in Europe, in *Geothermics and Geothermal Energy*, pp. 17–25, eds Cermak, V. & Haenel, R. E. Schweizerbartsche Verlagsbuchhandlung (Nagele U. Obermiller), Stuttgart.

Chen, C-Y., Chen, W-P & Molnar, P., 1980. The uppermost mantle *P*-wave velocities beneath Turkey and Iran, *Geophys. Res. Lett.*, **7**, 77–80.

Crampin, S., 1970. The disperion of surface waves in multilayered anisotropic media, *Geophys. J. R. astr. Soc.*, **21**, 387–402.

Crampin, S., 1978. Seismic wave propagation through a cracked solid: polarization as a possible dilatancy diagnostic, *Geophys. J. R. astr. Soc.*, **53**, 467–496.

Crampin, S., 1981. A review of wave motion in anisotropic and cracked elastic-media, *Wave Motion*, **3**, 343–391.

Crampin, S., S., 1984. Effective anisotropic elastic elastic constants for wave propagation through cracked solids, *Geophys. J. R. astr. Soc.*, **76**, 135–145.

Crampin, S. & Booth, D. C., 1985. Shear-wave polarizations near the north Anatolian fault—II. Interpretation in terms of crack-anisotropy, *Geophys. J. R. astr. Soc.*, **83**, 75–92.

Crampin, S. & Taylor, D. B., 1971. The propagation of surface waves in anisotropic media, *Geophys. J. R. astr. Soc.*, **25**, 71–87.

Der, Z. A. & Landisman, M., 1972. Theory for errors, resolution, and separation of unknown variables in inverse problems, with application to the mantle and the crust in southern Africa and Scandinavia, *Geophys. J. R. astr. Soc.*, **27**, 137–178.

Dewey, J. F. & Sengor, A. M. C., 1979. Aegean and surrounding regions: complex multiplate and continuum tectonics in a convergent zone, *Geol. Soc. Am. Bull.*, **90**, 84–92.

Dewey, J. F., Hempton, M. R., Kidd, W. S. F., Saroglu, F. & Sengor, A. M. C., 1986. Shortening of continental lithosphere: the neotectonics of eastern Anatolia—a young collision zone, in *Collision Tectonics. Geol. Soc. Special Pub.*, **19**, 3–36, eds Coward, M. P. & Ries, A. C.

Dost, B., 1987. The NARS array, a seismic experiment in western Europe, *PhD thesis*, Institute of Earth Sciences, Netherlands.

Dziewonski, A., Bloch, S. & Landisman, M., 1969. A technique for the analysis of transient seismic signals, *Bull. seism. Soc. Am.*, **59**, 427–444.

Ezen, U., 1983. Kuzey ve dogu Anadolu'da Zone dalgalarinin dispersiyonu ve yerkabugu yapisi (in Turkish), *Deprem Aras. Bulteni*, **43**, 42–62.

Foose, R. M., 1985. Geological information from satellite surveys of the Mediterranean region, in *Geological Evolution of the Mediterranean Basin*, pp. 33–53, eds. Stanley, D. J. & Wezel, F-C.

Forsyth, D. W., 1975. A new method for the analysis of multi-mode surface wave dispersion; application to Love wave propagation in the east Pacific, *Bull. seism. Soc. Am.*, **65**, 323–342.

Hudson, J. A., 1981. Wave speeds and attenuation of elastic waves in material containing cracks, *Geophys. J. R. astr. Soc.*, **64**, 133–150.

Hwang, H-J. & Mitchell, B. J., 1987. Shear velocities, Q_β, and the frequency dependence of Q_β in stable and tectonically active regions from surface wave observations, *Geophys. J. R. astr. Soc.*, **90**, 575–613.

Jackson, J. & McKenzie, D., 1984. Active tectonics of the Alpine–Himalayan belt between western Turkey and Pakistan, *Geophys. J. R. astr. Soc.*, **77**, 185–264.

Jackson, J. & McKenzie, D., 1988. The relationship between plate motions and seismic moment tensors, and the rates of active deformation in the Mediterranean and Middle East, *Geophys. J.*, **93**, 45–73.

Kanamori, H. & Abe, K., 1968. Deep structure of island arcs as revealed by surface waves, *Bull. Earthq. Res. Inst. Tokyo Univ.*, **46**, 1001–1025.

Kasapoglu, K. E. & Toksoz, M. N., 1983. Tectonic consequences of the collision of the Arabian and Eurasian plates: finite element models, *Tectonophysics*, **100**, 71–95.

Knopoff, L., Mueller, S. & Pilant, W. L., 1966. Structure of the crust and upper mantle in the Alps from the phase velocity of Rayleigh waves, *Bull seism. Soc. Am.*, **56**, 1009–1044.

Lawson, C. L. & Hanson, R. J., 1974. *Solving Least Squares Problems*, Prentice-Hall, New Jersey.

Le Pichon, X. & Angelier, J., 1979. The Hellenic arc and trench system: a key to the neotectonic evolution of the eastern Mediterranean, *Tectonophysics*, **60**, 1–42.

McEvilly, T. V., 1964. Central US crust–upper mantle structure from Love and Rayleigh wave phase velocity inversion, *Bull. seism. Soc. Am.*, **54**, 1997–2015.

McKenzie, D., 1972. Active tectonics of the Mediterranean region, *Geophys. J. R. astr. Soc.*, **30**, 109–185.

McKenzie, D., 1978. Active tectonics of the Alpine–Himalayan belt: the Aegean Sea and surrounding regions, *Geophys. J. R. astr. Soc.*, **55**, 217–254.

Mitchell, B. J., 1984. On the inversion of Love- and Rayleigh-wave dispersion and implications for Earth structure and anisotropy, *Geophys. J. R. astr. Soc.*, **76**, 233–241.

Nataf, H-C., Nakanishi, I. & Anderson, D. L., 1986. Measurements of mantle wave velocities and inversion for lateral heterogeneities and anisotropy, 3. Inversion, *J. geophys. Res.*, **91**, 7261–7307.

Panza, G. F., Mueller, St. & Calcagnile, G., 1980. The gross features of the lithosphere–asthenosphere system in Europe from seismic surface waves and body waves, *Pageoph*, **118**, 1209–1213.

Rotstein, Y. and Kafka, A. L., 1982. Seismotectonics of the southern boundary of Anatolia, eastern Mediterranean region: subduction, collision, and arc jumping, *J. geophys. Res.*, **87**, 7694–7706.

Rotstein, Y. & Ben-Avraham, Z., 1986. Active tectonics in the eastern Mediterranean: the role of oceanic plateaus and accreted terranes, *Israel J. Earth Sci.*, **35**, 23–39.

Russell, D. R., 1987. Multi-channel processing of dispersed surface waves, *PhD dissertation*, St Louis University, St Louis, MO.

Russell, D. R., Herrmann, R. B. & Hwang, H-J., 1984. SURF: an interactive set of surface wave dispersion programs for analyzing crustal structure, *Earthq. Notes,* **55,** 13.

Sengor, A. M. C. & Yilmaz, Y., 1981. Tethyan evolution of Turkey: a plate tectonic approach, *Tectonophysics,* **75,** 181–241.

Talwani, M., Sutton, G. H. & Worzel, J. L., 1959. A crustal section across the Puerto Rico trench, *J. geophys. Res.*, **64,** 1545–1555.

Turkelli, N., 1985. Seismic investigations of the crustal structure in central Anatolia, *PhD dissertation,* Middle East Technical University, Ankara, Turkey.

Yu, G-K. & Mitchell, B. J., 1979. Regionalized shear velocity models of the Pacific upper mantle from observed Love and Rayleigh wave dispersion, *Geophys. J. R. astr. Soc.,* **57,** 311–341.